Detecting entangled states in graphene via crossed Andreev reflection

Colin Benjamin and Jiannis K. Pachos
Quantum Information Group, School of Physics and Astronomy, University of Leeds, Woodhouse Lane, Leeds LS2 9JT, United Kingdom
(Received 18 July 2008; revised manuscript received 1 October 2008; published 1 December 2008)

Shot-noise cross correlations across single layer graphene structures are calculated with insulators separating a superconducting region. A different feature of specular crossed Andreev reflection comes into play due to the unique band structure of graphene. This gives rise to a rich structure in the states of the electric current flowing across the graphene sheet. We identified a parametric regime where *positive* shot-noise cross correlations of the current appear signifying entanglement. In contrast to previous proposals the sign of the cross correlations can be easily tuned by the application of a gate voltage.

DOI: 10.1103/PhysRevB.78.235403 PACS number(s): 73.23.−b, 72.70.+m, 03.65.Ud, 74.45.+c

I. INTRODUCTION

Shot noise is defined as the temporal fluctuation of electric current in a nonequilibrium setup.[1,2] When the shot-noise cross correlations between two regions turn positive it signals the presence of electronic entangled states.[3] In order to make use of these correlations for quantum information purposes one would need to spatially separate the electrons without destroying the entanglement.[4,5] This is ideally detected by entangled electrons traversing different wires.[6] The quantum correlations can be provided by Cooper pairs present in superconductors, which is the most entangled state found in nature.

To intuitively understand how shot noise contains the signature of entanglement we resort to statistics. Shot-noise cross correlations are defined as cross correlations of current fluctuations across two distinct regions. Absence of entanglement leads to positive correlations for photons (bunching) and negative for electrons (antibunching). The observation of positive shot-noise correlations for electrons is a signature that they are in an entangled state. This has been most famously predicted in normal metal-superconductor-normal metal structures,[1,2,4] but it has not yet been experimentally demonstrated. An earlier experimental attempt[7] in a two-dimensional electron gas beam splitter connected to a superconductor could not arrive at any definite conclusion possibly due to the low tunability of these devices. In this work we investigate what happens to the noise cross correlations when a single layer of graphene replaces the normal metal or semiconductor. Our motivation comes from the following fact. In contrast to a normal metal, the energy of transported electrons can be very efficiently controlled in a graphene layer via the application of a gate voltage thus being much more amenable to experiments. This was demonstrated in Ref. 8 where it was shown that the Josephson current could be very efficiently tuned via the application of a small gate voltage. We expect that this characteristic of graphene structures will facilitate the observation of entanglement in solid-state systems, thus, opening the way for their wider use in quantum information applications.[9]

II. MODEL

Graphene is a monatomic layer of graphite with a honeycomb lattice structure[10] that can be split into two triangular sublattices A and B. The electronic properties of graphene are effectively described by the Dirac equation.[11] The presence of isolated Fermi points, K_+ and K_-, in its spectrum, gives rise to two distinctive valleys. In this work we deal with a normal-insulator-superconductor-insulator-normal (NISIN) graphene junction. We consider a sheet of graphene on the x-y plane. Superconductivity is induced via the proximity effect, where a normal superconductor at close range on top of the sheet generates the desired superconducting correlations. In Fig. 1 we sketch our proposed system. The superconducting region is located between $0<x<L$, while the insulators are located on its left, $-d<x<0$, and on its right, $L<x<L+d$. The normal graphene planes are to the left end, $x<-d$, and to the right end, $x>L+d$.

As we will demonstrate in the following there are additional processes occurring at the normal graphene-superconducting graphene-normal graphene junctions than those seen at normal metal-superconductor-normal metal junctions.[12] These are local specular Andreev reflection and crossed (nonlocal) specular Andreev reflection. Importantly, Andreev reflection in graphene can switch the valley bands, i.e., conduction to valley; see Fig. 2. This process is known as specular Andreev reflection[13] explained in Fig. 2. In the

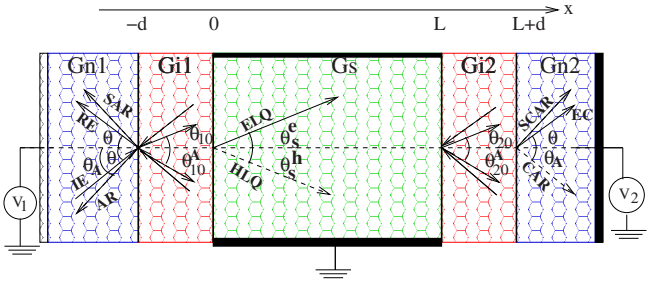

FIG. 1. (Color online) An overview of the setting from the top. Two insulating layers of graphene (Gi's) on either side of the superconducting graphene layer (Gs). Voltages V_1 and V_2 are applied to either end of the normal graphene layers (Gn's). Schematic of specular crossed Andreev reflection is also depicted. Incident electron at angle θ (IE). Reflected electron at angle $-\theta$ (RE). Andreev reflected hole at angle θ_A (AR). Specular Andreev reflected hole at angle $-\theta_A$ (SAR). Electronlike quasiparticle (ELQ). Holelike quasiparticle (HLQ). Crossed Andreev reflection at angle θ_A (CAR). Specular crossed Andreev reflected hole at angle $-\theta_A$ (SCAR). Electron cotunneling at angle θ (EC).

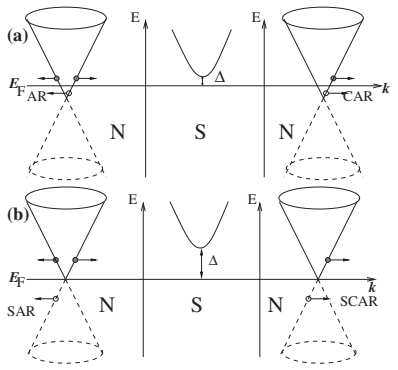

FIG. 2. Energy-momentum diagram to explain specular crossed Andreev reflection where the regions of normal (N) graphene and superconducting (S) graphene are as indicated. (a) $E_F > \Delta$ regime where Andreev and crossed Andreev reflection occur in the same band, and (b) $E_F \ll \Delta$ regime where Andreev and crossed Andreev reflection occur in a specular fashion across the bands. If, $E > E_F > \Delta$, where E is the energy of the particle measured from the Fermi level, then also specular Andreev reflection occurs. In all calculations we are in the regime where $E < \Delta$.

process of normal Andreev reflection, an incident electron from the normal metal side is reflected as a hole which retraces the trajectory of the electron. In specular Andreev reflection, the reflected hole follows the trajectory that a normally reflected electron would have. In this work we see, in addition to this, the possibility of specular crossed Andreev reflection, where a hole is reflected at the other lead but in a specular fashion (see Fig. 1).

For a quantitative analysis we describe our system by the Dirac–Bogoliubov–de Gennes equation that assumes the form[11]

$$\begin{pmatrix} \hat{H} - E_F\hat{I} & \Delta\hat{I} \\ \Delta^\dagger\hat{I} & E_F\hat{I} - \hat{T}\hat{H}\hat{T}^{-1} \end{pmatrix}\Psi = E\Psi, \tag{1}$$

where E is the excitation energy, Δ is the superconducting gap of a s-wave superconductor, Ψ is the wave function, and $\hat{\cdot}$ represents 4×4 matrices. In the above equation,

$$\hat{H} = \begin{pmatrix} H_+ & 0 \\ 0 & H_- \end{pmatrix}, \quad H_\pm = -i\hbar v_F(\sigma_x\partial_x \pm \sigma_y\partial_y) + U. \tag{2}$$

Here $\hbar, v_F$ (set equal to unity henceforth) are the Planck's constant and the energy independent Fermi velocity for graphene, while the σ's denote Pauli matrices that operate on the sublattices A or B. U is the electrostatic potential which can be adjusted independently via a gate voltage or doping. We assume $U=0$, in the normal regions, while $U=V_i, i=1,2$, in either insulating regions and $U=-U_0$ in the superconductor. The subscripts of Hamiltonian $\pm$ refer to the valleys of K_+ and K_- in the Brillouin zone. $T=-\tau_y\otimes\sigma_y C$ (C being complex conjugation) is the time reversal operator, with τ being Pauli matrices that operate on the $\pm$ space and $\hat{I}$ is the identity matrix.

Let us consider an incident electron from the normal side of the junction ($x<-d$) with energy E. For a right-moving electron with an incident angle θ the eigenvector and corresponding momentum read

$$\psi_+^e = [1, e^{i\theta}, 0, 0]^T e^{ip^e \cos\theta x}, \quad p^e = (E + E_F). \tag{3}$$

A left-moving electron is described by the substitution $\theta \to \pi - \theta$. If Andreev reflection takes place, a left-moving hole is generated with energy E and angle of reflection θ_A, and its corresponding wave function is given by

$$\psi_-^h = [0, 0, 1, e^{-i\theta_A}]^T e^{-ip^h \cos\theta_A x}, \quad p^h = (E - E_F). \tag{4}$$

The superscript e (h) denotes an electronlike (holelike) excitation. Since translational invariance in the y direction holds the corresponding component of momentum is conserved. This condition allows for the determination of the Andreev reflection angle θ_A through $p^h \sin(\theta_A) = p^e \sin(\theta)$. There is no Andreev reflection and consequently no subgap conductance for angles of incidence above the critical angle $\theta_c = \sin^{-1}(|E - E_F|/(E+E_F))$. In the insulators, $-d<x<0$ and $L<x<L+d$, the eigenvector and momentum of a right-moving electron are given by

$$\psi_{iI+}^e = [1, e^{i\theta_{i0}}, 0, 0]^T e^{ip_I^e \cos\theta_{i0} x}, \quad p_{iI}^e = (E + E_F - V_i), \tag{5}$$

with $i=1,2$ while a left-moving hole is described by

$$\psi_{iI-}^h = [0, 0, 1, e^{-i\theta_{i0}^A}]^T e^{-ip_{iI}^h \cos\theta_{i0}^A x}, \quad p_{iI}^h = (E - E_F + V_i). \tag{6}$$

On the superconducting side of the system, ($0<x<L$), the possible wave functions for transmission of a right-moving quasiparticle with excitation energy $E>0$ read

$$\Psi_{S+}^e = [u, ue^{i\theta^+}, v, ve^{i\theta^+}]^T e^{iq^e \cos\theta^+ x},$$

$$\Psi_{S-}^h = [v, ve^{i\theta^-}, u, ue^{i\theta^-}]^T e^{iq^h \cos\theta^- x}, \tag{7}$$

with $q^e = (E_F + U_0 + \sqrt{E^2 - \Delta^2})$ and $q^h = (E_F + U_0 - \sqrt{E^2 - \Delta^2})$. In the subgap regime the quasiparticle wave vectors have a small imaginary component as $q^{e/h} = E_F + U_0 \pm 1/\xi$, where $\xi = 1/\Delta$ is the coherence length. The coherence factors are given by $u = \sqrt{(1 + \sqrt{1 - \Delta^2/E^2})/2}$ and $v = \sqrt{(1 - \sqrt{1 - \Delta^2/E^2})/2}$. We have also defined $\theta^+ = \theta_S^e$, $\theta^- = \pi - \theta_S^h$. The transmission angles θ_S^α for the electronlike and holelike quasiparticles are given by $q^\alpha \sin\theta_S^\alpha = p^e \sin\theta, \alpha = e, h$. In the following we limit ourselves to the regime where $U_0 \gg \Delta$, such that the mean-field conditions for superconductivity are satisfied. The trajectories of the quasiparticles in the insulating region are defined by the angles θ_{i0} and θ_{i0}^A. These angles are related to the injection angles by

$$\sin\theta_{i0}/\sin\theta = (E + E_F)/(E + E_F - V_i),$$

$$\sin\theta_{i0}^A/\sin\theta = (E + E_F)/(E - E_F + V_i). \tag{8}$$

Here, we adopt the thin barrier limit defined as $\theta_{i0}, \theta_{i0}^A$ and $d \to 0$, while $V_i \to \infty$, such that $p_{iI}^e d, p_{iI}^h d \to \chi_i$. To solve the scattering problem, we match the wave functions at four interfaces: $\psi|x=-d = \psi_{1I}|_{x=-d}$, $\psi_{1I}|x=0 = \Psi_S|_{x=0}$, $\Psi_S|x=L$

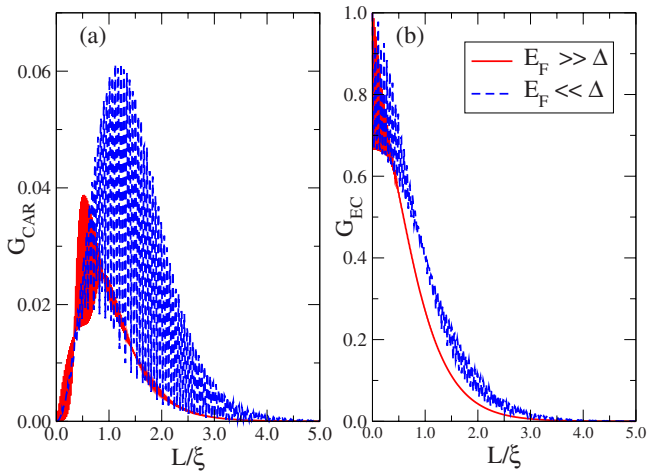

FIG. 3. (Color online) (a) Crossed Andreev reflection and (b) electronic cotunneling as function of the superconducting length, L/ξ. In both figures, $\chi_1=-\chi_2=\pi/4, U_0=1000\Delta$ and $E=0.15\Delta$.

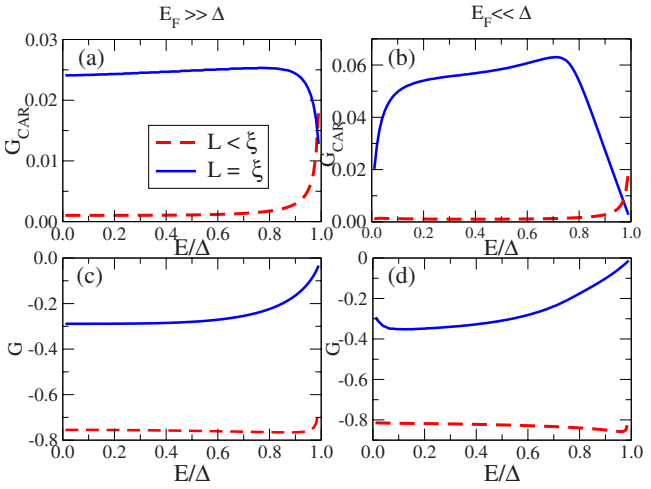

FIG. 4. (Color online) (a) Crossed Andreev reflection and (b) specular crossed Andreev reflection. Nonlocal conductance for a NISIN graphene based structure as function of the electronic energy for (c) normal and (d) specular reflection cases. In all figures, $\chi_1=-\chi_2=\pi/4$, and $U_0=1000\Delta$.

$=\psi_{2l}|_{x=L}$, and $\psi_{2l}|x=L+d=\psi|_{x=L+d}$, where, starting with normal graphene at left, $\psi=\psi_+^e+s_{11}^{ee}\psi_-^e+s_{11}^{eh}\psi_-^h$, $\psi_{il}=p_i\psi_{il+}^e+q_i\psi_{il-}^e+m_i\psi_{il+}^h+n_i\psi_{il-}^h, i=1,2$, $\Psi_S=p_S\Psi_{S+}^e+q_S\Psi_{S-}^e+m_S\Psi_{S+}^h+n_S\Psi_{S-}^h$, and finally for normal graphene at the right, $\psi=s_{12}^{ee}\psi_+^e+s_{12}^{eh}\psi_+^h$. Solving these equations leads to the amplitude of Andreev reflection s_{11}^{eh}, normal reflection s_{11}^{ee}, amplitude of electron cotunneling (EC) s_{12}^{ee}, and of crossed Andreev reflection (CAR) s_{12}^{eh}.

III. RESULTS

A. Specular crossed Andreev reflection

The first issue we tackle is the nonlocal conductance. Similar calculations, but for bipolar structures, were performed in Ref. 14. It is defined as the conductance in the right lead when both superconduction region and right graphene layer are grounded, while a voltage is applied to the left graphene sheet. The nonlocal conductance is given by the difference between the crossed Andreev and electronic cotunneling currents in the absence of a bias at right, where $G=G_{CAR}-G_{EC}$, with[12]

$$G_{CAR}=\int_{-\pi/2}^{\pi/2}d\theta\cos\theta_A|s_{12}^{eh}|^2,\quad G_{EC}=\int_{-\pi/2}^{\pi/2}d\theta\cos\theta|s_{12}^{ee}|^2. \tag{9}$$

In the following figures all the quantities are in their dimensionless form with the superconducting gap set to $\Delta=1$. The other energy parameters are expressed in terms of Δ. In Fig. 3 we plot the nonlocal CAR and EC current as function of the length of the superconducting region. We differentiate between two regimes. First, for $E_F\gg\Delta$ there is absence of interband nonlocal electron-hole transmission, denoted as the crossed Andreev regime (Fig. 2). Second, for $E_F\ll\Delta$ nonlocal interband electron-hole transmission is permitted giving rise to the specular crossed Andreev regime. As function of the length we find that both nonlocal coefficients vanish for large values. However, while the EC current decreases almost monotonically from a peak at $L\ll\xi$ to vanishing for $L\gg\xi$, the CAR current is maximum around $L\sim\xi$, and it vanishes for the extreme cases $L\ll\xi$, $L\gg\xi$. In Fig. 4, we plot the crossed Andreev current for normal transmission (left) as well as specular reflection (right). We observe that the specular CAR current might dominate the normal current in the $E\ll\Delta$ regime. One very interesting fact, which is partly seen in NS graphene junctions, is that just like the specular Andreev reflection seen there, here too the crossed specular Andreev reflection is reduced to vanishing at $E\sim\Delta$, but the normal crossed Andreev current is marginally reduced at $E\sim\Delta$. However, the nonlocal conductance (see Fig. 4) is dominated by electron cotunneling. It is also periodic as function of the strength of the insulating barrier's χ_i's (not plotted here).[15]

B. Shot-noise cross correlations

Next we calculate the shot-noise cross correlations, which is the main focus of our work. For that we first have to derive an expression for the shot noise in multiterminal settings[2] applied to graphene. The fluctuations of the current away from the average are termed noise. A general expression for current fluctuations between any two arbitrary leads is given by

$$N_{ij}(\tau)=\langle\Delta\hat{I}_i(t)\Delta\hat{I}_j(t+\tau)+\Delta\hat{I}_j(t+\tau)\Delta\hat{I}_j(t)\rangle, \tag{10}$$

where $\Delta\hat{I}_i(t)=\hat{I}_i(t)-\langle\hat{I}_i(t)\rangle$. The Fourier transform of Eq. (10) gives

$$N_{ij}(w)\delta(w+w')=\langle\Delta\hat{I}_i(w')\Delta\hat{I}_j(w)+\hat{I}_j(w)\Delta\hat{I}_i(w')\rangle. \tag{11}$$

For simplicity we consider the experimentally feasible zero-frequency noise limit, where displacement currents are absent. The current operator is given by

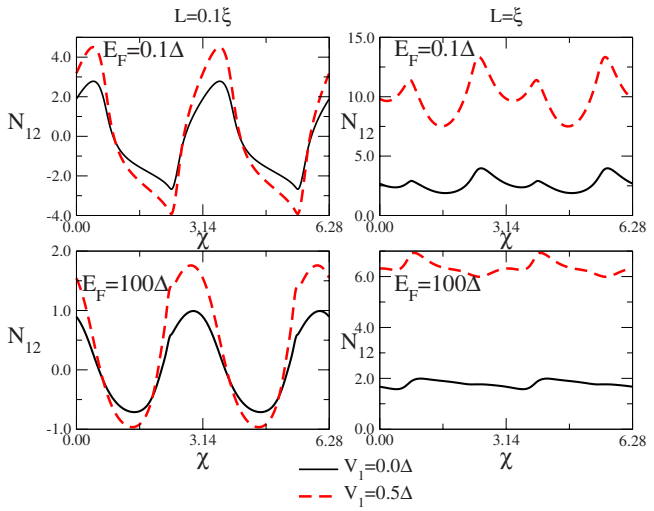

FIG. 5. (Color online) Noise cross correlations as function of the gate voltage ($\chi=\chi_1$) applied to the left insulator. The right insulator is fixed at gate voltage $\chi_2=0$, while $U_0=1000\Delta$ and $V_2=0.2\Delta$.

$$\hat{I}_i(w=0)=\sum_{\substack{k,l\in Gn_1,Gn_2,Gs\\ \alpha,\beta,\gamma,\delta\in e,h}} q_\alpha \int dE A_{k\gamma,l\delta}(i,\alpha)\hat{a}^\dagger_{k\gamma}\hat{a}_{l\delta}, \quad (12)$$

with $A_{k\gamma,l\delta}(i,\alpha)=\delta_{ik}\delta_{il}\delta_{\alpha\gamma}\delta_{\alpha\delta}-s^{\alpha\gamma\dagger}_{ik}s^{\alpha\delta}_{il}$, where Greek indices denote the nature (e for electrons, h for holes) of the incoming/outgoing particles with their associated charges q_α, while Latin indices l and k identify the graphene sheets and $\hat{a}_{l\delta}$ denotes annihilation operator for a particle in lead l with charge δ. From Eqs. (11) and (12) the zero-frequency noise cross correlations between the currents at left and right normal graphene sheets (Gn_1,Gn_2) become[2]

$$N_{12}=\sum_{\substack{k,l\in Gn_1,Gn_2,Gs\\ \alpha,\beta,\gamma,\delta\in e,h}} \frac{q_\alpha q_\beta}{h}\int_{-\pi/2}^{\pi/2} d\theta\cos\theta \int dE A_{k\gamma,l\delta}(1,\alpha) \times A_{l\delta,k\gamma}(2,\beta) f_{k\gamma}(1-f_{l\delta}). \quad (13)$$

$f_{k\gamma}$ is a Fermi function for particles of type γ in graphene sheet k.

In the limit $L\ll\xi$ Andreev and cross-Andreev reflection vanish, which implies that in this limit noise correlations are negative.[4] In the limit $L\gg\xi$ both nonlocal currents vanish leading to vanishing noise cross correlations. However, it is the length in between these limits where noise not only becomes substantial but also can change sign. In Fig. 5 we plot the shot-noise cross correlations as function of the gate voltage, which tunes the strength of the left insulator in the system. As the effective barrier strength changes, one sees negative cross correlations turning positive for $L<\xi$. This indicates that a gate voltage can tune the entanglement properties. More interesting is the case $L=\xi$, where noise cross correlations turn completely positive enabled by the strong CAR signal. In the specular regime the noise is enhanced. This can be understood from Fig. 3 where the CAR signal in the specular regime is double than that of the normal case. The behavior depicted in Fig. 5 is of significance for the experimental detection of entanglement in solid-state systems. It shows that a gate voltage can change the sign of noise cross correlations unlike that predicted for normal metal counterparts. It is worth mentioning that for $L\gg\xi$ the magnitudes of the noise cross correlations are very much reduced (not plotted) but one can also see completely positive noise cross correlations.

IV. CONCLUSIONS

Recent CAR experiments[16] are the next generation in detecting the splitting of Cooper pairs into different leads, thus probing entanglement in the context of nanophysics. In this work we provide the results of noise cross-correlation spectra as a function of gate voltage for a NISIN graphene junction. The Fano factor (not presented here) is also on predictable lines and shows a spike in case of enhanced positive noise cross correlations, indicating bunching. We point out the phenomenon of specular crossed Andreev reflection, which enhances noise cross correlations. The settings envisaged in this work are experimentally accessible. A typical s-wave superconductor like aluminum has a coherence length of $\xi=1600$ nm. Since the proximity effect induces superconducting correlations in graphene, an aluminum superconductor on top of the graphene layer would give rise to a similar correlation length. This separation would not be a challenge since crossed Andreev reflection measurements are carried out routinely at less than these lengths. Further, the superconducting gap in aluminum is 1 meV, while the typical Fermi energy in normal doped graphene is around 80 meV. In our study we have considered for certain situations $E_F=100\Delta$, i.e., $E_F\gg\Delta$, which corresponds to undoped graphene, while $E_F\ll\Delta$ can be tuned via doping graphene or by a grate voltage. These values are realistic and thus obviate any reasons for skepticism. Employing these entangled states for quantum information processing will increase the allure of graphene.

ACKNOWLEDGMENTS

We would like to thank Chris Marrows and Graham Creeth for stimulating discussions. This work was supported by EPSRC-GB, the EU grants EMALI and SCALA, and the Royal Society.

[1] G. B. Lesovik, T. Martin, and G. Blatter, Eur. Phys. J. B **24**, 287 (2001).
[2] M. P. Anantram and S. Datta, Phys. Rev. B **53**, 16390 (1996).
[3] C. W. J. Beenakker and C. Schonenberger, Phys. Today **56** (5), 37 (2003).
[4] R. Melin, C. Benjamin, and T. Martin, Phys. Rev. B **77**, 094512 (2008).
[5] P. Samuelsson and M. Büttiker, J. Low Temp. Phys. **146**, 115 (2007).
[6] P. Recher, E. V. Sukhorukov, and D. Loss, Phys. Rev. B **63**, 165314 (2001).
[7] B. R. Choi, A. E. Hansen, T. Kontos, C. Hoffmann, S. Oberholzer, W. Belzig, C. Schonenberger, T. Akazaki, and H. Takayanagi, Phys. Rev. B **72**, 024501 (2005).
[8] H. B. Heersche *et al.*, Nature (London) **446**, 56 (2007).
[9] C. W. J. Beenakker and M. Kindermann, Phys. Rev. Lett. **92**, 056801 (2004).
[10] C. W. J. Beenakker, arXiv:0710.3848 (unpublished).
[11] J. Linder and A. Sudbo, Phys. Rev. Lett. **99**, 147001 (2007).
[12] S. Duhot and R. Mélin, Eur. Phys. J. B **53**, 257 (2006); G. Deutscher and D. Feinberg, Appl. Phys. Lett. **76**, 487 (2000); J. M. Byers and M. E. Flatte, Phys. Rev. Lett. **74**, 306 (1995); C. Benjamin, Phys. Rev. B **74**, 180503(R) (2006).
[13] C. W. J. Beenakker, Phys. Rev. Lett. **97**, 067007 (2006); Rev. Mod. Phys. **80**, 1337 (2008).
[14] J. Cayssol, Phys. Rev. Lett. **100**, 147001 (2008).
[15] S. Bhattacharjee and K. Sengupta, Phys. Rev. Lett. **97**, 217001 (2006).
[16] D. Beckmann, H. B. Weber, and H. v. Löhneysen, Phys. Rev. Lett. **93**, 197003 (2004); S. Russo, M. Kroug, T. M. Klapwijk, and A. F. Morpurgo, *ibid.* **95**, 027002 (2005); P. Cadden-Zimansky and V. Chandrasekhar, *ibid.* **97**, 237003 (2006).